

CONSTRAINT OF SIDE-GROOVE AND ITS INFLUENCE ON FRACTURE TOUGHNESS PARAMETER IN CHARPY-SIZE SPECIMENS

X.P. ZHANG and Y.W. SHI

*Department of Mechanical Engineering,
Xi'an Jiaotong University, Xi'an, Shaanxi Province,
The People's Republic of China*

ABSTRACT

This paper has studied the effect of side-groove constraint on pre-cracked Charpy-size specimen, and the influence of side-groove on fracture toughness parameters. The results indicate that when side-groove depth approach a critical value, the maximum load toughness J_m values are nearly coincident with the initiation toughness J_i values. Thickening action of side-groove may be expressed by calculating the additional thickness of specimen. For different materials the additional thickness due to side-groove is distinct. When the side-groove depth is 33% of specimen thickness the specimen obtains the maximum additional thickness. The side-groove constraint coefficient (C) presented by this paper can quantitatively evaluate the level of plastic constraint at crack tip, and explain the experimental results well.

KEYWORDS

Side-groove, Charpy-size specimen, fracture toughness, constraint coefficient

INTRODUCTION

Charpy-size specimens are usually used in surveillance program of nuclear reactor power station pressure vessel by neutron radiated embrittlement. Especially in recent years, using pre-cracked Charpy-size specimen with side-groove to evaluate fracture toughness of materials has been researched and paid much attention [1~10]. This method not only satisfies the demand of small size specimen in surveillance test of fracture toughness, but also could avoid complicated physical methods used to monitor the initial conditions of crack propagation. For most materials this method solved the problem in which the small size specimen did not satisfy the valid condition of fracture toughness measurement. Furthermore, pre-cracked Charpy-size specimens is cheap and save materials. Comparing with the standard specimen, the side-groove of pre-cracked Charpy-size specimen has changed the stress distribution at crack tip along the whole thickness direction of specimen. The regions of through-thickness deformation is restricted. In order to determine fracture toughness conveniently and economically, Ritchie et al. [1,3] has proposed that the fracture toughness of maximum load at load vs load-point displacement curve is regarded as the initiation fracture toughness. However, some results of a mild steel have indicated that slow crack propagation exceeded 1 mm if fracture toughness of maximum load was regarded as the critical value of initiation and the

side-groove depth reached to 40-60% of specimen thickness[2]. In this studies the crack initiation point is estimated by the compliance changing rate from the load vs load-point displacement curve so as to investigate how the fracture toughness of maximum load point (J_m) approaches that of initiation point (J_i) with increasing side-groove depth. This paper also researches the influence of side-groove of pre-cracked Charpy-size specimen upon fracture toughness parameters and effect of side-groove on through-thickness direction constraint of specimen, and discusses the relationship among the constraint coefficient and critical side-groove depth as well as critical J-integral value.

TEST MATERIAL AND PROCEDURE

Material and Specimen Preparation. The materials for test are heavy-section nuclear pressure vessel steels A508CL3-A and A508CL3-B produced by two works as well as BHW35 steel. The chemical composition and mechanical properties of test materials are given in tables 1 and 2.

Table 1 Chemical composition of test materials (w.t.%)

Materials	C	Mn	Si	S	P	Ni	Cr	Mo	V	Cu	Al
A508CL3-A	0.14	1.29	0.27	0.006	0.004	0.98	0.05	0.51	0.03		
A508CL3-B	0.20	1.29	0.24	0.007	0.008	0.75	0.06	0.50	0.004	0.08	0.012
BHW35	0.14	1.32	0.34	0.012	0.019	0.86	0.39	0.27			

Table 2 Mechanical properties of test materials

Materials	σ_y (MPa)	σ_{UTS} (MPa)	δ_5 (%)	Φ (%)	Strain hardening exponent	Hv
A508CL3-A	540	642	22	73	6.5	220~230
A508CL3-B	515	650	24	66	6.9	245~255
BHW35	586	664	25	68	8.0	260-275

The pre-cracked Charpy-size specimen is shown in Fig.1(a) and the direction is in L-S. The length of fatigue crack (a/W) is 0.45~0.55. After pre-cracked the side-grooves with different depth were machined on the both sides of specimens in the shape of V notch and with root radius of 0.1 mm, as shown in Fig.1(b).

Experimental Procedure. Test was carried out in an Instron 1195 electronic tensile testing machine with loading speed of 0.5mm/min at room temperature. The span of supports was 40mm. During the testing process curve of the load vs load-point displacement was recorded. When load reached to the maximum point, the specimen was unloaded, and then the speci-

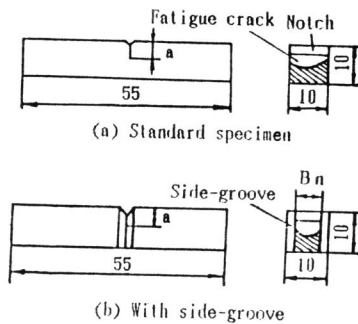


Fig.1 Pre-cracked Charpy-size specimen.

mens were broken at liquid nitrogen temperature. The initial crack length (a_0) and grown crack length (Δa_m) corresponding to the maximum load were measured by means of 5 points average method. The relative depth of side-groove is defined as follows:

$$d_s = [(B - B_n) / B] \times 100\% \quad (1)$$

where B is the specimen thickness, and B_n is the net thickness of cross section of specimen, as shown in Fig.1(b). The maximum load absorbed energy, E_m , can be calculated from load vs load-point displacement curve, and the J-integral value of maximum load, J_m , can be expressed as:

$$J_m = 2E_m / [B_n(W - a_0)] \quad (2)$$

The elastic-plastic fracture toughness K_{Jc} can be evaluated by

$$K_{Jc} = \sqrt{E \cdot J_m / (1 - \nu^2)} \quad (3)$$

where E is the Young's modulus of elasticity, ν is the Poisson's ratio.

The compliance changing rate of specimen during loading process was used to determine the initiation point of crack growth. The compliance changing rate can be calculated by [11]:

$$\Delta C / C_e = (C - C_e) / C_e \quad (4)$$

where C_e is the elastic compliance, C is the assumed linear compliance at arbitrary point on load vs load-point displacement curve.

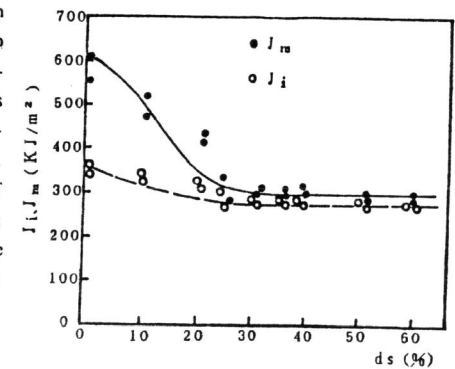
The valid elastic-plastic fracture toughness is estimated by means of method of J_R resistant curve of the National Standard of China, i.e. GB2038[12], which requires specimen size as follows: $B = 20\text{mm}$, $W = 24\text{mm}$, $S = 4W$, and bluntening line is $J = 3 \cdot \sigma_r \cdot \Delta a$.

RESULTS AND DISCUSSIONS

Effect of Side-groove Depth on Fracture Toughness Parameters. Fig.2 shows the results of J_m vs d_s . It is found that J_m values decrease rapidly when side-groove depth increase. As soon as the d_s reaches the critical value ($d_{s,c}$), J_m also achieve the critical value ($J_{m,c}$), and keeping constant. For a certain material, when d_s value is larger than ($d_{s,c}$) value, J_m value would keep constant, which is so-called platform value ($J_{m,p}$).

From the experimental results of A508CL3-A, A508CL3-B and BHW35 steels, the ($d_{s,c}$) are 25%, 30% and 20% respectively, the ($J_{m,c}$) are 302.4KJ/m², 269.3 KJ/m² and 148.0KJ/m² respectively, and the ($J_{m,p}$) are 300 ± 14.6KJ/m², 265.8 ± 10.8KJ/m² and 149.8 ± 12.8KJ/m² respectively.

Fig.3 shows the results of Δa_m changing



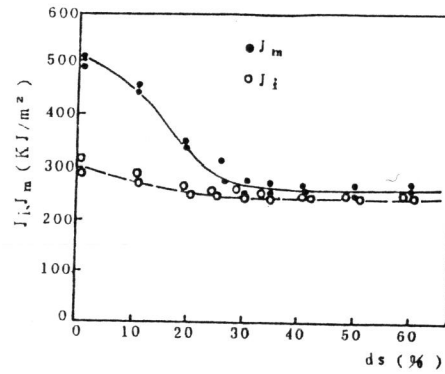
(a) A508CL3-A steel

with side-groove depth. When side-groove depth increases, the Δa_m values drop gradually, and the curve has no obvious turn point. At the critical depth of side-groove for A508CL3-A, A508CL3-B and BHW35 steels, Δa_m , the length of slow crack growth at maximum load point is 230 μ m, 234 μ m and 134 μ m respectively.

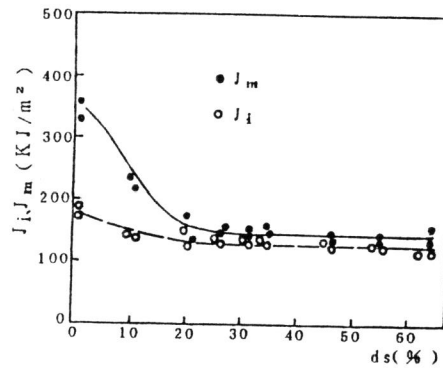
For pre-cracked Charpy-size specimens with side-grooves, slow crack growth is very short when side-groove depth get to the critical value $(d_s)_c$. For the specimens with critical side-groove depth, the slow crack growth is the 4.5%, 4.7% and 2.7% of the initial crack length a_0 for A508CL3-A, A508CL3-B and BHW35 steels respectively, where it is assumed that $a_0 = 5$ mm. It is clear that the crack growth is very small, and the maximum load point almost approaches the initiation.

In order to further confirm the above conclusion, the fracture toughness at initiation, J_i , calculated by means of compliance changing rate is also shown in Fig.2. The tendency of J_i vs d_s curve is the same as that of J_m vs d_s curve, but the curve of J_i vs d_s is lower and gentler. When $d_s > (d_s)_c$, J_i value keep constant, which is so-called platform value $(J_i)_p$. For A508CL3-A, A508CL3-B and BHW35 steels, $(J_i)_p$ values are 273.2 ± 6.7 KJ/m², 252.6 ± 9.2 KJ/m² and 138.6 ± 7.2 KJ/m² respectively. Thus, J_m value would gradually approach the fracture toughness at initiation J_i while d_s increases. When values of d_s reach and exceed the critical depth of side-groove, the ratio of (J_i/J_m) is approximately equal to one, as shown in Fig.4. It is shown that the fracture toughness at maximum load is nearly equal to that at initiation for pre-cracked Charpy-size specimens with deep side-grooves.

Constraint Effect of Side-groove and Constraint Coefficient. The side-grooves in a specimen is equivalent to thickening the specimen, and strengthening the level of stress triaxiality along the



(b) A508CL3-B steel



(c) BHW35 steel

Fig.2 Results of J_m or J_i vs side-groove depth.

thickness direction of the specimen. It also changes the stress state at crack tip, and make the mixture stress state in small Charpy-size specimen become more plane strain state. The research results on a ICrMoV steel indicated that [4,5] when side-groove depth of pre-cracked Charpy-size specimen was 20%, the region of plane strain got to 88% of the whole thickness of the specimen, by contrast, the region of plane strain of standard specimen was only 25% of the whole thickness of the specimen, i.e. in the center of specimen thickness there existed a narrow region of plane strain. The effect of side-groove on thickening pre-cracked Charpy-size specimen may be expressed in terms of equivalent thickness B_e as follows:

$$B_e = B_n [1 + 0.67(B_n/B)(1 - B_n/B)] \quad (5)$$

The curves of B_e and B_n changing with d_s are shown in Fig.5. Considering that the different materials have the different sensitivity to side-grooves, the equation (5) should be revised, and two parameters of material, that is, the strain hardening exponent n expressed by Ramberg-Osgood equation and the ratio of $(\sigma_y / \sigma_{UTS})$ are introduced as follows:

$$(B_e)_r = B_n [1 + 0.67(n\sigma_y / \sigma_{UTS})(B_n/B)(1 - B_n/B)] \quad (6)$$

where $(B_e)_r$ is the revised equivalent thickness. According to Equation (6), the curves of $(B_e)_r$ and B_n changing with d_s are shown in Fig.6. If both sides of the Equation (6) minus B_n ,

$$\Delta B = (B_e)_r - B_n = 0.67 B_n (n\sigma_y / \sigma_{UTS}) [(B_n/B) - (B_n^2/B^2)] \quad (7)$$

where ΔB is the additional thickness of the specimens caused by constraint effect of side-grooves. Then, we calculate the first derivation of ΔB with respect to B_n for Equation (7), and the extreme value:

$$d(\Delta B) / dB_n = 1.34(B_n/B) - 2.01(B_n/B)^2 = 0$$

Therefore, as B_n equals 6.67mm, i.e. d_s equals 33% of the specimen thickness, the maximum additional thickness of pre-cracked Charpy-size specimen is obtained, as shown in Fig.6. For A508CL3-A, A508CL3-B and BHW35 steels, the maximum values of additional thickness are 5.4mm, 5.3mm and 9.4mm respectively, and the equivalent thickness are 12.1mm, 12.0mm and 16.1mm respectively. It is found that the effect of side-groove constraint is explicit in specimens. In order to evaluate the level of plastic constraint of side-grooves at crack tip, and make the constraint effect of side-grooves quantitative and convenient, effect of side-groove constraint can be

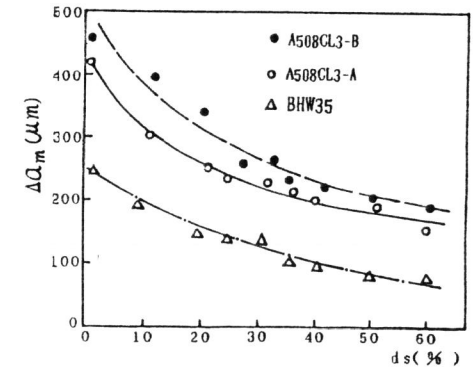


Fig.3 Results of Δa_m vs side-groove depth.

expressed in terms of constraint coefficient(C). For pre-cracked Charpy-size specimen with side-grooves C can be written as follows:

$$C = P_m \cdot S / [B_n \cdot W^2 \cdot \sigma_{UTS} \cdot (1 - a/W)^2] \quad (8)$$

where P_m is the maximum load of load vs load-point displacement curve. Relation of C changing with d_s is shown in Fig.7. It is found that as side-groove depth increase, C values also increase gradually, i.e. the plastic constraint increases. When side-groove depth reaches and exceeds the critical value ($d_{s,c}$), C values would keep constant. The critical J-integral values depend upon the stress state at crack tip. For the pre-cracked Charpy-size specimen with side-grooves, C values can be used to evaluate stress state under the action of side-groove constraint quantitatively. That C values keeps constant means the stress state is steady along the thickness direction of specimen. Correspondently, the critical J-integral values keep constant, it is due to constancy of C values that result in the critical J-integral values keeping steady. The experimental results proved the above.

The Comparison Between J_m and Valid Elastic-plastic Fracture Toughness. J_R resistant curves of A508CL3-A, A508CL3-B and BHW35 steels were measured, and the results of valid J_{IC} are shown in table 3. According to the slope of J_R resistant curves, the tearing modulus, T_M , can be obtained as follows:

$$T_M = (E / \sigma_f^2) (dJ / da) \quad (9)$$

The T_M values and the K_{JC} values converted from valid J_{IC} by equation (3) are also shown in table 3. In table 3, J_m values corresponding to critical side-groove depth of pre-cracked Charpy-size specimen and the K_{JC} values converted from the J_m are also listed to compare

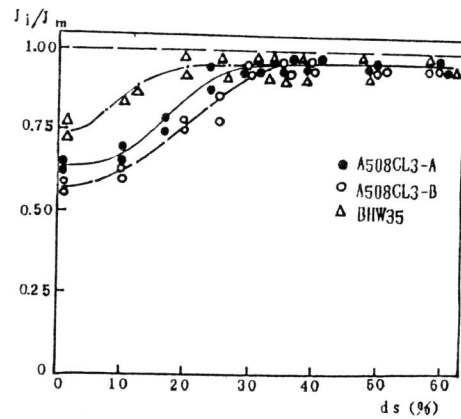


Fig.4 Results of the ratio of (J_1 / J_m) vs d_s .

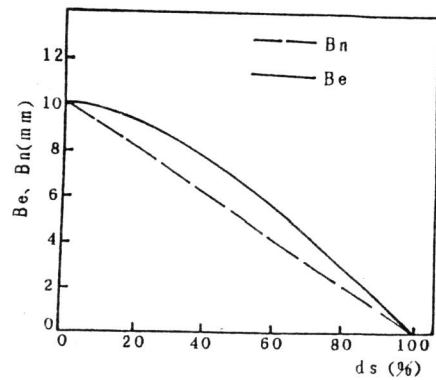


Fig.5 Curves of B_e and B_n vs d_s .

Table 3 The comparison between valid J_{IC} (K_{JC}) and J_m (converted K_{JC})

Materials	Valid J_{IC}	Valid K_{JC} ($MN / m^{3/2}$)	T_M	$(J_m)_c$	K_{JC} [Converted from $(J_m)_c$]
A508CL3-A	322.4	270.1	331.0	303.1	262.8
A508CL3-B	304.7	262.6	305.3	269.0	247.6
BHW35	203.0	214.4	298.2	148.0	184.6

with the valid values of fracture toughness. It can be found that J_m values are a bit smaller than valid J_{IC} values. For A508CL3-A, A508CL3-B and BHW35 steels, the K_{JC} values converted from J_m values are smaller than valid K_{JC} values by 2%, 6% and 13.8% respectively. Nevertheless, according to the maximum load absorbed energy E_m , the conservative values of elastic-plastic fracture toughness of pressure vessel materials can be obtained by means of pre-cracked Charpy-size specimen with deep side-groove. This is a convenient single-specimen method that is especially suitable for embrittlement surveillance of nuclear pressure vessel due to neutron irradiation.

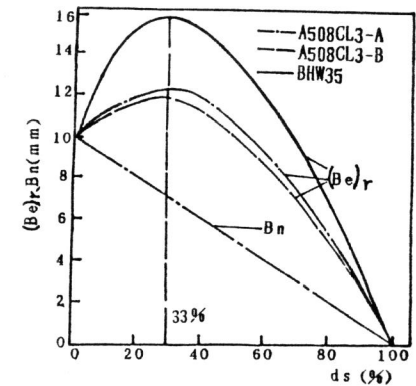


Fig.6 Curves of $(B_e)_r$ and B_n vs d_s .

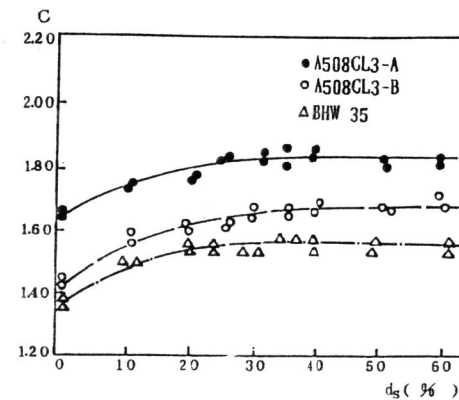


Fig.7 Relation of C changing with d_s .

CONCLUSION

- (1) When the side-groove depth is larger than the critical value $(d_s)_c$, the J_m values would almost equal to the J_i values, and the P_m point nearly coincides with the fracture initiation point on the load vs load-point displacement curve.
- (2) Constraint of the side-grooves may be evaluated by means of constraint coefficient(C) values quantitatively while side-groove depth changes.
- (3) Side-grooves have the action of thickening the specimen, and for a certain material there exist an optimal side-groove depth of which specimen gains the maximum additional thickness.
- (4) The critical value of side-groove depth, $(d_s)_c$, determined by curves of J_m vs d_s are the same as that determined through curves of C vs d_s . In fact, the tendency of J_m vs d_s depend upon that of C value vs d_s .
- (5) According to the maximum load absorbed energy of load vs load-point displacement curve, the conservative values of elastic-plastic fracture toughness can be obtained. This small size single-specimen method is especially suitable for embrittlement surveillance of fracture toughness of nuclear pressure vessel due to neutron irradiation.

Acknowledgement—The authors greatly acknowledge the financial support from the National Nuclear Safety Bureau of China

REFERENCES

- [1] R.O.Ritchie, W.L.Server and R.A.Wullaert, International Journal of Fracture, 14(1978),R139–142.
- [2] A.A.Willoughby, International Journal of Fracture, 15(1979), R125–126.
- [3] W.L. Server, R.A. Wullaert and R.O. Ritchie, Journal of Engineering Materials and Technology, Transactions of ASME, 102(1980),192–199
- [4] B.K.Neale, International Journal of Pressure Vessel and Piping, 10(1982),375–398.
- [5] B.K.Neale, International Journal of Pressure Vessel and Piping,12(1983),207–227.
- [6] ASTM E185–82, Standard Practice for Conducting Surveillance Tests for Light-water cooled Nuclear power Reactor Vessels, E706(1F), ASTM, Philadelphia, 1982.
- [7] ASTM E636–83, Standard practice for Conducting Supplemental Surveillance Tests for Nuclear Power Reactor Vessels, E706(1H), ASTM, Philadelphia, 1983.
- [8] T.Varga, and D.H. Njo, Selection of specimen types for irradiation surveillance programs, Radiation Embrittlement and Surveillance of Nuclear Reactor Pressure Vessels, ASTM STP819, 1983, pp.166–173.
- [9] L.M.Davies and T.Ingham, Overview of studies in the United Kingdom on neutron irradiation embrittlement of pressure vessel steels, Radiation Embrittlement of Nuclear Reactor Pressure Vessel Steels, ASTM STP909, 1986, pp.13–33.
- [10] R.Ahlstrand, K.Toironen, M.Valo, and B.Bars, Surveillance programmes and irradiation embrittlement research of the Loviisa nuclear power plant, *ibid*, pp.55–69.
- [11] M.K. Tseng, and H.L. Marcus, Engineering Fracture Mechanics, 16,895–930(1982).
- [12] GB2038–82, Test Method of Fracture Toughness of Ductile Metallic Materials by Means of J_R Resistant Curve, the National Standard of China, 1982.